Wolff et al. 2011

Strontium isotopes and magma dynamics: insights from Snake River-type rhyolite

GSA data rep. Number 2011277

Table DR1: Summary table of data for the Snake River-type rhyolites

Unit	Bulk SiO_2 (wt.%)	$^{87}Sr/^{86}Sr$ max	$^{87}Sr/^{86}Sr$ min	$^{87}Sr/^{86}Sr$ average	Sample location
Shoshone Falls Rhyolite	70.3-70.7	0.71158	0.71115	0.71134	42.5982, -114.4673
Balanced Rock Lava	70.0-72.5	0.71259	0.71223	0.71246	42.5455, -114.9563
Dorsey Creek Lava	72.0-74.2	0.71246	0.71197	0.71223	42.25, -115.55
Tuff of City of Rocks	69.9-70.8	0.71331	0.71255	0.71311	43.1409, -114.6548
Tuff of Gwin Springs	71.9-74.6	0.71258	0.71231	0.71247	43.1424, -114.9348
Tuff of Thorn Creek	72.0-74.7	0.71344	0.71304	0.71322	41.1666, -114.9917
Pole Creek Vitrophyre	73.0-75.3	0.71081	0.71030	0.71055	43.1681, -114.9842
Tuff of Knob	71.4-72.4	0.70986	0.70932	0.70964	43.2110, -114.9947
Tuff of Fir Grove	74.9-77.0	0.71069	0.71022	0.71036	43.2068, -115.0034
Rhyolite of Deer Springs	74.6-75.3	0.71080	0.71006	0.71043	43.2078, -114.9666

LA-MC-ICPMS $^{87}Sr/^{86}Sr$ isotope analysis

Samples were analysed on a ThermoFinnigan Neptune MC-ICPMS, using a New Wave UP-213 Nd-YAG laser at Washington State University using methods described by Ramos et al. (2004). Laser power was varied throughout the analysis period to maintain a fluence of 11-13 J/cm^2. During analysis the stage was raised by 2 microns per pass to maintain the focus of laser onto the newly ablated surface of the sample. Troughs were 80 µm wide and ≥600 µm long meaning that the 100 isotope ratios collected and averaged to derive a final value were collected from between 2 and 4 passes. In samples with low Sr contents trough widths were increased to 120 µm. Speed of passes was 30 µm /second and the sample surface was cleaned by pre-ablation. Sr intensities were corrected for Kr and Rb interferences and the resulting interference-corrected Sr isotope ratios exponentially corrected for mass bias to $^{86}Sr/^{88}Sr = 0.1194$. We have not found it necessary to correct for contributions from doubly-charged Er and Yb when analyzing plagioclase. Two in-house plagioclase standards with known $^{87}Sr/^{86}Sr$ ratios of 0.70405 and 0.70671 respectively were used to monitor daily drift.

Table DR2: Full results from LA-ICPMS isotope determinations, errors quoted include those on the standard

Deer Springs		
BE SRP 09 015 / 016	$^{87}Sr/^{86}Sr$	1 std err
09 016 g1 c1	0.71038	0.00012
09 016 g3 r1	0.71025	0.00012
09 016 g3 r2	0.71047	0.00011
09 016 g4 r1	0.71042	0.00012
09 016 g4 r2	0.71065	0.00011
09 016 g4 r3	0.71047	0.00011
09 016 g5 r1	0.71046	0.00012
09 016 g5 r2	0.71016	0.00010
09 016 g5 c incs	0.71028	0.00013
09 015 g1 r1	0.71065	0.00012
09 015 g1 c1	0.71080	0.00012
09 015 g2 r1	0.71076	0.00010
09 015 g2 r2	0.71054	0.00011
09 015 g2 c1	0.71059	0.00011
09 015 g3 r1	0.71058	0.00011
09 015 g3 r2	0.71050	0.00011
09 015 g3 c1	0.71030	0.00010
09 015 g4 r1	0.71009	0.00010
09 015 g4 c1	0.71006	0.00010
09 015 g5 r1	0.71010	0.00012
09 015 g5 c1	0.71030	0.00011
09 015 g6 r1	0.71080	0.00013
Average	**0.71043**	
Max	**0.71080**	
Min	**0.71006**	

Fir Grove UV		
BE SRP 09 017 / 021	$^{87}Sr/^{86}Sr$	1 std err
09 021 g1 r2	0.71038	0.00011
09 021 g1 r3	0.71033	0.00013
09 017 g1 r1	0.71029	0.00011
09 017 g1 r2	0.71038	0.00012
09 017 g1 c1	0.71037	0.00012
09 017 g2 r1	0.71030	0.00010
09 017 g2 r2	0.71022	0.00012
09 017 g3 r1	0.71036	0.00010
09 017 g3 r2	0.71028	0.00011
09 017 g4 r1	0.71069	0.00012
Average	**0.71036**	
Max	**0.71069**	
Min	**0.71022**	

Tuff of Knob

BE SRP 09 023 / 013	$^{87}Sr/^{86}Sr$	1 std err
09 023 g1 r1	0.70950	0.00010
09 023 g1 c1	0.70965	0.00011
09 023 g2 r1	0.70948	0.00011
09 023 g2 r2	0.70986	0.00012
09 023 g3 r1	0.70948	0.00012
09 023 g3 r2	0.70983	0.00014
09 023 g4 r1	0.70956	0.00010
09 023 g4 rc	0.70944	0.00010
09 023 g5 r1	0.70970	0.00010
09 013 g1 r1	0.70966	0.00009
09 013 g1 r2	0.70968	0.00011
09 013 g2 r1	0.70977	0.00009
09 013 g2 rc2	0.70974	0.00009
09 013 g3 r1	0.70979	0.00011
09 013 g3 r2	0.70974	0.00010
09 013 g3 c1	0.70979	0.00010
09 013 g3 c2	0.70962	0.00010
09 013 g4 r1	0.70965	0.00010
09 013 g4 r2	0.70962	0.00011
09 013 g5 r1	0.70971	0.00010
09 013 g6 c1	0.70932	0.00011
09 013 g6 c2	0.70942	0.00011

Tuff of Knob cont.	$^{87}Sr/^{86}Sr$	1 std err
09 013 g6 c3	0.70951	0.00012
09 013 g6 c4	0.70939	0.00009
09 013 g6 c5	0.70947	0.00009
09 013 g6 r1	0.70936	0.00011
09 013 g7 r1	0.70962	0.00011
09 013 g7 c1	0.70967	0.00011
09 013 g8 rc1	0.70969	0.00012
09 013 g9 r1	0.70980	0.00012
09 013 g9 c1	0.70972	0.00011
09 013 g10 r1	0.70969	0.00010
09 013 g10 c1	0.70976	0.00010
09 013 g11 c1	0.70964	0.00010
09 013 g12 r1	0.70970	0.00011
09 013 g13 r1	0.70981	0.00011
09 013 g14 r1	0.70977	0.00011
09 013 g15 r1	0.70966	0.00011
09 013 g16 r1	0.70964	0.00010
09 013 g16 c1	0.70958	0.00012
09 013 g17 r1	0.70967	0.00010
09 013 g18 r1	0.70976	0.00010
Average	**0.70964**	
Max	**0.70986**	
Min	**0.70932**	

Table DR2 cont.

Pole Creek Vitrophyre

BE SRP 09 009	$^{87}Sr/^{86}Sr$	1 std err
09 009 g1 r1	0.71075	0.00011
09 009 g2 r1	0.71030	0.00010
09 009 g2 c1	0.71047	0.00010
09 009 g3 r1	0.71047	0.00012
09 009 g3 c1 inc	0.71079	0.00012
09 009 g4	0.71045	0.00012
09 005 g5 r1	0.71046	0.00011
09 009 g7 r1	0.71046	0.00012
09 009 g8 r1	0.71054	0.00011
09 009 g8 c1	0.71047	0.00012
09 009 g8 r2	0.71055	0.00012
09 009 g9 r1	0.71062	0.00010
09 009 g9 r2	0.71081	0.00014
Average	**0.71055**	
Max	**0.71081**	
Min	**0.71030**	

Thorn Creek

BE SRP 09 010	$^{87}Sr/^{86}Sr$	1 std err
09 010 g1 r1	0.71332	0.00010
09 010 g1 r2	0.71344	0.00009
09 010 g1 r3	0.71342	0.00012
09 010 g1 c1	0.71335	0.00011
09 010 g2 r1	0.71312	0.00010
09 010 g2 r2	0.71327	0.00010
09 010 g2 c1	0.71312	0.00009
09 010 g3 r1	0.71331	0.00012
09 010 g3 c1	0.71331	0.00011
09 010 g4 r1	0.71334	0.00010
09 010 g4 c1	0.71335	0.00010
09 010 g4 r3	0.71313	0.00012
09 010 g5 r1	0.71306	0.00011
09 010 g5 c1	0.71315	0.00011
09 010 g6 r1	0.71328	0.00011
09 010 g6 c1	0.71325	0.00011
09 010 g7 r1	0.71322	0.00010
09 010 g8 r1	0.71318	0.00012
09 010 g8 c1	0.71344	0.00012
09 010 g9r1	0.71314	0.00009
09 010 g10 r1	0.71307	0.00009
09 010 g11 rc	0.71325	0.00010
09 010 g12 rc	0.71307	0.00010
09 010 g13 r1	0.71310	0.00012
09 010 g13 c1	0.71316	0.00013
09 010 g14 r1	0.71309	0.00011
09 010 g14 c1	0.71304	0.00010
09 010 g14 r2	0.71323	0.00011
09 010 g15 r1	0.71318	0.00012
Average	**0.71322**	
Max	**0.71344**	
Min	**0.71304**	

Table DR2 cont.

Gwin Springs

BE SRP 09 006	$^{87}Sr/^{86}Sr$	1 std err
09 006 g1 r1	0.71253	0.00009
09 006 g1 c1	0.71256	0.00012
09 006 g2 r1	0.71241	0.00009
09 006 g2 c1	0.71246	0.00009
09 006 g3 r1	0.71248	0.00010
09 006 g3 c1	0.71250	0.00010
09 006 g4 r1	0.71231	0.00009
09 006 g4 c1	0.71249	0.00009
09 006 g5 rc	0.71251	0.00009
09 006 g6 r1	0.71258	0.00010
09 006 g6 r2	0.71249	0.00010
09 006 g7 r1	0.71245	0.00009
09 006 g7 c1	0.71245	0.00011
09 006 g8	0.71249	0.00011
09 006 g9 r1	0.71237	0.00010
Average	**0.71247**	
Max	**0.71258**	
Min	**0.71231**	

City of Rocks

BE 09 028	$^{87}Sr/^{86}Sr$	1 std err
09 028 g1 r1	0.71299	0.00009
09 028 g1 c1	0.71302	0.00010
09 028 g2 r1	0.71318	0.00010
09 028 g2 c1	0.71288	0.00010
09 028 g3 r1	0.71314	0.00009
09 028 g3 c1	0.71313	0.00010
09 028 g4 r1	0.71287	0.00008
09 028 g4 r2	0.71299	0.00010
09 028 g4 r3	0.71320	0.00010
09 028 g4 c1	0.71316	0.00010
09 028 g5 r1	0.71323	0.00009
09 028 g6 r1	0.71306	0.00010
09 028 g6 r2	0.71301	0.00010
09 028 g7 r1	0.71310	0.00009
09 028 g7 c1	0.71329	0.00009
09 028 g8 r1	0.71324	0.00009
09 028 g8 c1	0.71324	0.00009
09 028 g9 r1	0.71311	0.00009
09 028 g9 c3	0.71331	0.00009
09 028 g10 r1	0.71311	0.00011
09 028 g10 c1	0.71326	0.00012
09 028 g11 r1	0.71316	0.00010
09 028 g11 c1	0.71324	0.00009
09 028 g12 r1	0.71299	0.00013
09 028 g12 c1	0.71303	0.00011
09 028 g13 r1	0.71318	0.00012
09 028 g14 c1	0.71255	0.00010
09 028 g15 r1	0.71318	0.00010
09 028 g15 c1	0.71307	0.00010
Average	**0.71311**	
Max	**0.71331**	
Min	**0.71255**	

Table DR2 cont.

Dorsey Creek rhyolite

	$^{87}Sr/^{86}Sr$	1 std err
dcg1 r1	0.71218	0.00016
dcg2 r1	0.71197	0.00016
dcg3 c1	0.71231	0.00014
dcg4 c1	0.71230	0.00013
dcg4r1	0.71212	0.00010
dcg5 r1	0.71207	0.00012
dc g6 r1	0.71213	0.00013
dcg7r1	0.71232	0.00012
dcc g8 r1	0.71230	0.00013
dc g8 r2	0.71232	0.00012
dc g8 c1	0.71217	0.00012
dc g9 r1	0.71240	0.00013
dcg10 r1	0.71217	0.00009
dc g10 r2	0.71227	0.00010
dc g11 r1	0.71246	0.00010
Average	**0.71223**	
Max	**0.71246**	
Min	**0.71197**	

Balanced Rock Lava

	$^{87}Sr/^{86}Sr$	1 std err
BRL g1 r1	0.71259	0.00011
BRL g2 c1	0.71250	0.00013
BRL g3 r1	0.71246	0.00013
BRL g4 r1	0.71251	0.00012
BRL g5 r1	0.71243	0.00013
BRL g6 r1	0.71256	0.00011
BRL g7 r1	0.71247	0.00012
BRL g7 c1	0.71241	0.00011
BRL g8 r1	0.71249	0.00011
BRL g8 c1	0.71258	0.00012
BRL g9 r1	0.71248	0.00012
BRL g9 c1	0.71248	0.00012
BRL g10 r1	0.71253	0.00012
BRL g10 c1	0.71243	0.00013
BRL g11 r1	0.71247	0.00014
BRL g12 r1	0.71223	0.00012
BRL g13 r1	0.71234	0.00014
Average	**0.71246**	
Max	**0.71259**	
Min	**0.71223**	

Shoshone Falls Rhyolite Lava

	$^{87}Sr/^{86}Sr$	1 std err
I3425 g1 r1	0.71129	0.00014
I3425 g2 r1	0.71130	0.00015
I3425 g3 r1	0.71134	0.00014
I3425 g3 c1	0.71120	0.00016
I3425 g4 r1	0.71153	0.00013
I3425 g5 r1	0.71115	0.00013
I3425 g6 r1	0.71134	0.00013
I3425 g7 c1	0.71158	0.00014
Average	**0.71134**	
Max	**0.71158**	
Min	**0.71115**	

Table DR2 cont.

Davis Mtn basalt

BE SRP 09 024	$^{87}Sr/^{86}Sr$	1 std err
09 024 g1 r1	0.70891	0.00012
09 024 g2 r1	0.70877	0.00012
09 024 g3 r1	0.70922	0.00012
09 024 g4 r1	0.70922	0.00014
09 024 g4 c1	0.70885	0.00012
09 024 g5 r1	0.70932	0.00013
09 024 g5 r2	0.70928	0.00014
09 024 g6 r1	0.70939	0.00012
09 024 g6 c1	0.70916	0.00014
09 024 g7 r1	0.70919	0.00013
09 024 g7 c1	0.70919	0.00013
09 024 g8 r1	0.70863	0.00011
09 024 g8 c1	0.70869	0.00013
09 024 g9 r1	0.70990	0.00015
09 024 g9 c1	0.70971	0.00012
09 024 g10 r1	0.70938	0.00014
09 024 g10 c1	0.70926	0.00012
09 024 g11 r1	0.70900	0.00015
09 024 g11 c1	0.70905	0.00013
09 024 g12 r1	0.70957	0.00011
09 024 g12 c1	0.71017	0.00012
09 024 g12 r2	0.70980	0.00011
09 024 g13 r1	0.70967	0.00012
09 024 g14 c1	0.70921	0.00014
09 024 g14 r1	0.70966	0.00014
Average	**0.70929**	
Max	**0.71017**	
Min	**0.70863**	

McHan basalt

BE 09 037	$^{87}Sr/^{86}Sr$	1 std err
09 037 g1 r1	0.70649	0.00010
09 037 g1 c1	0.70630	0.00010
09 037 g2 r1	0.70614	0.00011
09 037 g2 c1	0.70631	0.00010
09 037 g3 r1	0.70632	0.00010
09 037 g3 c1	0.70618	0.00010
09 037 g4 r1	0.70648	0.00011
09 037 g4 c1	0.70639	0.00011
09 037 g5 c1	0.70654	0.00012
09 037 g6 r1	0.70753	0.00007
09 037 g7 r1	0.70744	0.00007
09 037 g7 c1	0.70563	0.00010
09 037 g8 r1	0.70619	0.00009
09 037 g9 c1	0.70620	0.00009
09 037 g9 c2	0.70567	0.00008
09 037 g8 c1	0.70748	0.00008
09 037 g7 rc	0.70585	0.00008
09 037 g10 r1	0.70585	0.00009
09 037 g10 c1	0.70587	0.00008
09 037 g10 r2	0.70697	0.00008
09 037 g11 c1	0.70672	0.00008
Average	**0.70641**	
Max	**0.70753**	
Min	**0.70563**	

Table DR2 cont.

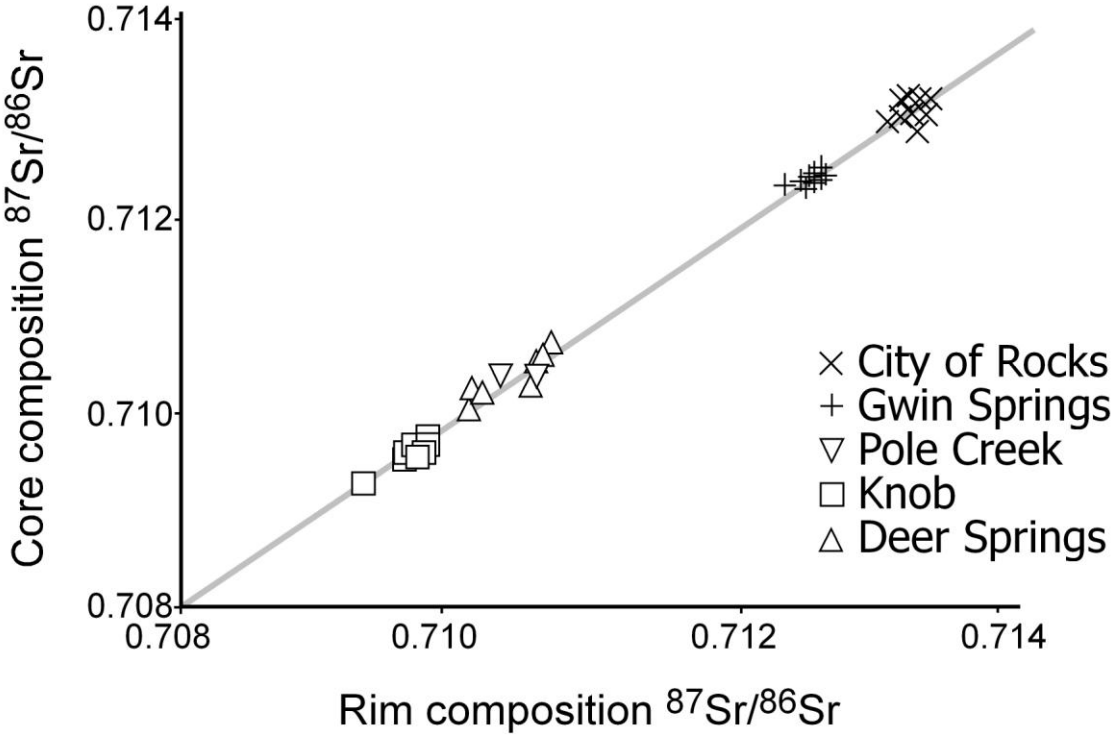

Figure DR1: Isotope ratios of rims and cores of plagioclase grains measured via LA-ICPMS. The grey line represents 1:1 ratio of rim:core.

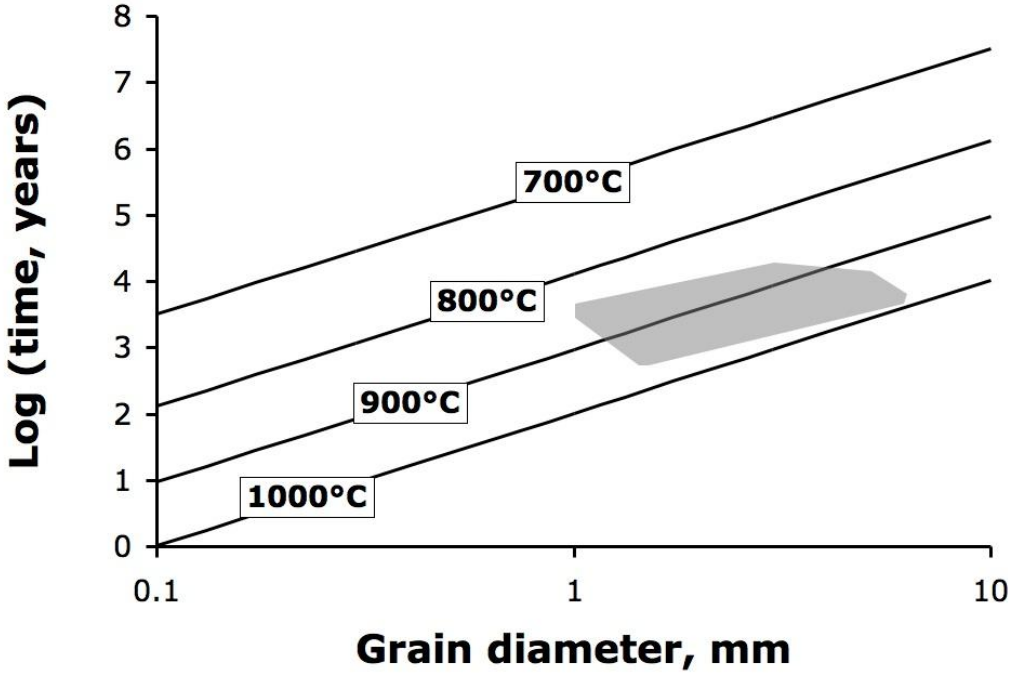

Figure DR2. Effective Sr isotope diffusional equilibration times for An_{30} plagioclase at 4 different temperatures, using the diffusion coefficients of Giletti and Casserly (1994). The time for the center of a grain radius *r* to achieve 90% equilibration (which we take as the limit of what we can effectively measure) is given by $Dt/r^2 = 0.3$, where *D* is the diffusion coefficient and *t* is time (Crank, 1975, p.91 and Fig. 6.1). Gray shaded field is the range of effective equilibration times for the high-temperature rhyolite units in Figure 2, using temperatures yielded by mineral geothermometers (Cathey and Nash, 2009; Ellis, 2009; Ellis et al., 2010).

References for data in Figure DR2:

Cathey, H.E. and Nash, B.P. 2009, Pyroxene thermometry of rhyolite lavas of the Bruneau–Jarbidge eruptive center, Central Snake River Plain: Journal of Volcanology and Geothermal Research, v. 188, p. 173-185, doi:10.1016/j.jvolgeores.2009.05.024

References for data in Figure 4:

Anderson, A.T., Jr. and Brown, G.G. 1993, CO_2 contents and formation pressures of some Kilauean melt inclusions: American Mineralogist, v. 78, p. 794-803.

Anderson, A.T., Jr., Newman, S., Williams, S.N., Druitt, T.H., Skirius, C. and Stolper, E., 1989, H_2O, CO_2, Cl, and gas in Plinian and ashflow Bishop rhyolite: Geology, v. l7, p. 221-225

Arce, J.L., Cervantes, K.E., Macias, J.L. and Mora, J.C., 2005, The 12.1 ka Middle Toluca Pumice: a dacitic Plinian-subplinian eruption of Nevado de Toluca in central Mexico: Journal of Volcanology and Geothermal Research, v.147, p. 125-143.

Bacon, C.R., Newman, S. and Stolper, E., 1992, Water, CO_2, Cl, and F in melt inclusions in phenocrysts from three Holocene explosive eruptions, Crater Lake, Oregon: American Mineralogist, v. 77, p. 1021-1030.

Belkin, H.E., De Vivo, B., Török, K. and Webster, J., 1998, Pre-eruptive volatile content, melt-inclusion chemistry, and microthermometry of interplinian Vesuvius lavas (pre-A.D. 1631): Journal of Volcanology and Geothermal Research, v. 82, p. 79-95, doi:10.1016/S0377-0273(97)00058-9.

Benjamin, E.R., Plank, T., Wade, J.A., Kelley, K.A., Hauri, E.H. and Alvarado, G.E., 2007, High Water Contents in Basaltic Magmas from Irazú Volcano, Costa Rica: Journal of Volcanology and Geothermal Research, v. 168 1-4: 68-92.

Blundy, J. and Cashman, K., 2005, Rapid decompression-driven crystallisation recorded by melt inclusions from Mount St. Helens volcano: Geology, v. 33, p. 793-796.

Coombs, M.L. and Gardner, J.E., 2001, Shallow storage conditions for the rhyolite of the 1912 eruption at Novarupta, Alaska: Geology, v. 29, p. 775-778, DOI 10.1130/0091-7613(2001)029.

Costa, F., Scaillet, F. and Pichavant, M., 2004, Petrological and Experimental Constraints on the Pre-eruption Conditions of Holocene Dacite from Volca´n San Pedro (36S, Chilean Andes) and the Importance of Sulphur in Silicic Subduction-related Magmas: Journal of Petrology, v. 45, p. 855-881.

Crank, K., 1975, The mathematics of diffusion (2nd edition). Oxford University Press, 414 p.

Dunbar, N.W. and Hervig, R.L., 1992, Volatile and trace element composition of melt inclusions from the lower Bandelier Tuff, implications for magma chamber processes and eruptive style: Journal of Geophysical Research 97 B11:15,129-15,150

Dunbar, N.W., Hervig, R.L. and Kyle, P.K., 1989, Determination of pre-eruptive H_2O, F and Cl contents of silicic magmas using melt inclusions: Examples from Taupo volcanic center, New Zealand: Bulletin of Volcanology, v. 51, p. 177-184.

Gurenko, A.A., Belousov, A.B., Trumbull, R.B. and Sobolev, A.V., 2005, Explosive basaltic volcanism of the Chikurachki Volcano (Kurile arc, Russia): Insights on pre-eruptive magmatic conditions and volatile budget revealed from phenocryst-hosted melt inclusions and groundmass glasses: Journal of Volcanology and Geothermal Research, v. 147, p. 203-232.

Johnson, E.M. and Rutherford, M.J., 1989, Experimentally Determined Conditions in the Fish Canyon Tuff, Colorado, Magma Chamber: Journal of Petrology v. 30 p. 711-737.

Mandeville, C.W., Webster, J.D., Tappen, C., Taylor, B.E., Timbal, A., Sasaki, A., Hauri, E. and Bacon, C.R. 2009, Stable isotope and petrologic evidence for open-system degassing during the climactic and pre-climactic eruptions of Mt. Mazama, Crater Lake, Oregon: Geochimica Cosmochimica Acta, v. 73, p. 2978-3012.

Manley, C.R., 1996b, Morphology and maturation of melt inclusions in quartz phenocrysts from the Badlands rhyolite lava flow, southwestern Idaho: American Mineralogist v. 81, p. 158-168.

Michaud, V., Clocchiatti, R. and Sbrana, S., 2000, The Minoan and post-Minoan eruptions, Santorini (Greece) in the light of melt inclusions: chlorine and sulphur behavior: Journal of Volcanology and Geothermal Research, v. 99 p. 195-214.

Roggensack, K., 2001, Unraveling the 1974 eruption of Fuego volcano (Guatemala) with small crystals and their young melt inclusions: Geology, v. 29, p. 911-914.

Roggensack, K., Hervig, R.L., McKnight, S.B. and Williams, S.N., 1997, Explosive Basaltic Volcanism from Cerro Negro Volcano: Influence of Volatiles on Eruptive Style. Science v. 277, p. 1639-1642.

Saito, G., Kazahaya, K., Shinohara, H., Stimac, J. and Kawanabe, Y., 2001, Variation of volatile concentration in a magmatic system of Satsuma-Iwojima volcano deduced from melt inclusions: Journal of Volcanology and Geothermal Research, v. 108, p. 11-31.

Schmitt, A.K., 2001, Gas-saturated crystallization and degassing in large-volume, crystal-rich dacitic magmas from the Altiplano-Puna, northern Chile: Journal of Geophysical Research, v. 106, p. 30561-30578.

Smith, V.C., Shane, P., Nairn, I.A. and Williams, C.M., 2006, Geochemistry and magmatic properties of eruption episodes from Haroharo linear vent zone, Okataina Volcanic Centre, New Zealand during the last 10 kyr: Bulletin of Volcanology, v. 69, p. 57-88.

Stix, J. and Layne, G., 1996, Gas saturation and evolution of volatile and light lithophile elements in the Bandelier magma chamber between two caldera-forming eruptions: Journal of Geophysical Research, v. 101, p. 25181-25196.

Suh, C.E., Luhr, J.F. and Njome, M.S., 2008, Olivine-hosted glass inclusions from Scoriae erupted in 1954–2000 at Mount Cameroon volcano, West Africa: Journal of Volcanology and Geothermal Research, v. 169, p. 1-33.

Troll, V.R. and Schmincke, H.-U., 2002, Magma mixing and crustal recycling recorded in ternary feldspar from compositionally zoned peralkaline ignimbrite 'A', Gran Canaria, Canary Islands: Journal of Petrology, v. 43, p. 243-270.

Webster, J.D., Burt, D.M. and Aguillon, R.A., 1996, Volatile and lithophile trace-element geochemistry of Mexican tin rhyolite magmas deduced from melt inclusions: Geochimica Cosmochimica Acta, v. 60, p. 3267-3283.

Webster, J.D., De Vivo, B. and Tappen, C., 2003, Volatiles, magmatic degassing and eruptions of Mt. Somma-Vesuvius: Constraints from silicate melt inclusions, Cl and H_2O solubility experiments and modeling: In: De Vivo, B. and Bodnar, R.J., (eds.) Melt inclusions in volcanic systems: methods, applications and problems. Elsevier

Webster, J.D. and Duffield, W.A., 1991, Volatiles and lithophile elements in Taylor Creek Rhyolite: constraints from glass inclusion analysis: American Mineralogist, v. 76, p. 1628-1645.

Wilson, C.J.N., Blake, S., Charlier, B.L.A. and Sutton, A.N., 2006, The 26.5 ka Oruanui eruption, Taupo volcano, New Zealand: development, characteristics and evacuation of a large rhyolitic magma body: Journal of Petrology, v. 47, p. 35-69.

Wolff, J.A., Balsley, S.D. and Gregory, R.T., 2002, Oxygen isotope disequilibrium between quartz and sanidine from the Bandelier Tuff, New Mexico, consistent with a short residence time of phenocrysts in rhyolitic magma: Journal of Vocanology and Geothermal Research, v. 116, p. 119-135.